Molecular Biology of the Cell
Vol. 18, 1312–1323, April 2007

Apical Epidermal Growth Factor Receptor Signaling: Regulation of Stretch-dependent Exocytosis in Bladder Umbrella Cells

Elena M. Balestreire and Gerard Apodaca

Laboratory of Epithelial Cell Biology, Departments of Medicine and Cell Biology and Physiology, University of Pittsburgh, Pittsburgh, PA 15261

Submitted September 21, 2006; Revised January 18, 2007; Accepted January 29, 2007
Monitoring Editor: Keith Mostov

The apical surface of polarized epithelial cells receives input from mediators, growth factors, and mechanical stimuli. How these stimuli are coordinated to regulate complex cellular functions such as polarized membrane traffic is not understood. We analyzed the requirement for growth factor signaling and mechanical stimuli in umbrella cells, which line the mucosal surface of the bladder and dynamically insert and remove apical membrane in response to stretch. We observed that stretch-stimulated exocytosis required apical epidermal growth factor (EGF) receptor activation and that activation occurred in an autocrine manner downstream of heparin-binding EGF-like growth factor precursor cleavage. Long-term changes in apical exocytosis depended on protein synthesis, which occurred upon EGF receptor-dependent activation of mitogen-activated protein kinase signaling. Our results indicate a novel physiological role for the EGF receptor that couples upstream mechanical stimuli to downstream apical EGF receptor activation that may regulate apical surface area changes during bladder filling.

INTRODUCTION

The apical plasma membrane of epithelial cells is a dynamic sensory organelle that receives and responds to extracellular stimuli such as ATP, hormones, growth factors, and mechanical stimuli such as hydrostatic pressure and shear stress (Karnaky, 1998). These stimuli act through apically expressed receptors, channels, and transporters to modulate the growth, protein synthesis, division, differentiation, and apoptosis of the subjacent epithelial tissues (Alberts, 2002). In addition, these stimuli can increase membrane turnover (i.e., exocytosis/endocytosis) at the apical surface of the epithelial cells, thereby modulating the surface area of the apical plasma membrane, the receptor/channel/transporter content of this membrane domain, and the ability of the cell to respond to extracellular signals. At present, the association among extracellular mediators, mechanical stimuli, and apical membrane dynamics is poorly understood.

The epidermal growth factor (EGF) receptor (EGFR), a member of the ErbB family of receptor tyrosine kinases (including EGFR/ErbB1, ErbB2, ErbB3, and ErbB4), is an important regulator of mechanotransduction, cell signaling, and membrane traffic (Barbieri *et al*., 2000; Holbro and Hynes, 2004; Tschumperlin *et al*., 2004). The ErbB family of receptors can be activated upon binding of one of 10 ligands, which differentially interact with ErbB1, ErbB3, and ErbB4 receptors (ErbB2 has no known ligands) (Holbro and Hynes, 2004). The ligands are synthesized as transmembrane precursors that are released upon cleavage by metalloproteinases (Harris *et al*., 2003). Ligands activate ErbB receptors in an autocrine, paracrine, or juxtacrine manner (Singh and Harris, 2005), and receptor activation can be initiated downstream of mechanical stimuli. Ligand binding induces the hetero- and/or homodimerization of receptors and subsequent autophosphorylation of tyrosine residues within their cytoplasmic tails. In turn the phosphorylated tyrosine residues act as docking sites for signaling proteins, which dictate activation of downstream signaling pathways including the mitogen-activated protein kinase (MAPK) cascades (Olayioye *et al*., 2000). MAPKs include extracellular signal-regulated kinase (ERK)1/2, p38 kinase, c-Jun NH_2-terminal kinase (JNK), and ERK5, and they are known to cause changes in protein expression through regulation of transcription (Pearson *et al*., 2001).

Although EGFR is generally thought to be a basolateral receptor, EGFR is found at the apical surface of mouse eight-cell stage embryos, enterocytes lining the suckling rat ileum, and gastric mucosal oxyntic cells (Gonnella *et al*., 1987; Wiley *et al*., 1992; Chen *et al*., 2002). In many cases, the function of apical EGFR is unknown, but in oxyntic cells, EGF, acting through the EGFR, has a long-term effect of decreasing paracellular permeability and increasing the barrier to mucosal acid production (Chen *et al*., 2002). Intriguingly, when EGFR is overexpressed in LLC-PK1 cells, a fraction of the receptor is mistargeted to the apical cell surface where it can stimulate downstream signaling cascades (Kuwada *et al*., 1998), indicating that EGFRs may generally have the ability to signal via apical epithelial surfaces. Several studies have described the expression of EGFR and ErbB family members (with various localization patterns) in normal human uroepithelium, the stratified transitional epithelium that lines the renal pelvis and mucosal surface of the ureters and bladder, and their increased mu-

This article was published online ahead of print in *MBC in Press* (http://www.molbiolcell.org/cgi/doi/10.1091/mbc.E06–09–0842) on February 7, 2007.

Address correspondence to: Gerard Apodaca (gla6@pitt.edu).

Abbreviations used: BFA, brefeldin A; EGF, epidermal growth factor; EGFR, epidermal growth factor receptor; HB-EGF, heparin-binding epidermal growth factor-like protein.

cosal surface expression during cancerous states (Messing, 1990; Chow *et al*., 1997; Rotterud *et al*., 2005). However, the function of EGFR in normal uroepithelial physiology is not well understood.

Extracellular signaling events modulate membrane traffic in umbrella cells, the outermost cell layer of the uroepithelium. The apical surface area of umbrella cells is highly dynamic, and it is postulated that discoidal/fusiform-shaped vesicles that underlie the apical surface are inserted and retrieved during bladder filling and voiding (Lewis and de Moura, 1982; Truschel *et al*., 2002). Apical exocytosis in these cells is governed by Ca^{2+}; cAMP; the cytoskeleton (Lewis and de Moura, 1984; Truschel *et al*., 2002; Wang *et al*., 2003); and extracellular stimuli, including mechanical stretch (Lewis and de Moura, 1984; Wang *et al*., 2005), ATP (Wang *et al*., 2005), and adenosine (Yu *et al*., 2006). Intriguingly, in addition to ErbB1–4, multiple ErbB receptor ligands are also expressed in the uroepithelium (Mellon *et al*., 1996; Freeman *et al*., 1997). Although tyrosine kinases are known to be important in mechanotransduction in other cell types such as vascular endothelial cells, keratinocytes, and osteoblasts (Takahashi *et al*., 1997; Rezzonico *et al*., 2003; Yano *et al*., 2004), the role that tyrosine phosphorylation, in general, and the ErbB receptors, in particular, play in umbrella cell exocytosis is unknown.

In this report, we provide evidence that stretch-induced exocytosis in umbrella cells is dependent on EGFR signaling initiated at the apical pole of the cells. Stretch of isolated uroepithelium resulted in the rapid activation of EGFR, and stretch-induced exocytosis was blocked by treatment with an EGFR-selective inhibitor or function-blocking antibodies when added to the mucosal but not serosal surfaces of the tissue. EGFR activation was mediated by an autocrine mechanism that was prevented by addition of antibodies to heparin-binding EGF-like growth factor (HB-EGF) or treatment with a broad-spectrum metalloproteinase inhibitor. Stretch and EGFR ligand-induced increases in surface area were sensitive to cycloheximide and inhibitors of MAPK signaling pathways. Our data indicate a novel physiological role for the EGFR that links mechanotransduction, EGFR activation at the apical pole of the umbrella cell, and protein synthesis downstream of MAPK activation to stimulate exocytosis at the apical pole of polarized umbrella cells.

MATERIALS AND METHODS

Reagents and Antibodies

All reagents were obtained from Sigma-Aldrich unless otherwise specified. Pharmacological agents were prepared as stock solutions in the following diluents: cycloheximide (10 mg/ml in sterile distilled water), genistein (10 mM in dimethyl sulfoxide [DMSO]), AG-1478 (25 μM in DMSO; Calbiochem, San Diego, CA), AG-1296 (25 mM in DMSO; Calbiochem), AG-490 (30 mM in DMSO; Calbiochem), PP2 (25 μM in DMSO; Calbiochem), AG-9 (25 μM in DMSO; Calbiochem), brefeldin-A (BFA; 5 mg/ml in ethanol), GM-6001 (10 mM in DMSO; Calbiochem), GM-6001 negative control (10 mM in DMSO; Calbiochem), U0126 (10 mM in DMSO; Cell Signaling Technology, Beverly, MA), PD-098059 (10 mM in DMSO), SB-203580 (10 mM in DMSO; Calbiochem), JNK inhibitor II (500 μM in DMSO; Calbiochem), and CRM-197 (5 mg/ml in distilled H_2O). Stock solutions of EGFR ligands were prepared as follows: EGF (100 μg/ml in phosphate-buffered saline [PBS] with 0.1% bovine serum albumin [BSA]), HB-EGF (100 μg/ml in PBS with 0.1% BSA), heregulin-β (100 μg/ml in PBS with 30% glycerol), and transforming growth factor (TGF)-α (25 μg/ml in sterile distilled water; Chemicon International, Temecula, CA). The EGFR antibody #2232 (Cell Signaling Technology) was used at 1:200 for immunofluorescence. EGF-fluorescein isothiocyanate (FITC) (40 μg/ml concentration; Invitrogen, Carlsbad, CA) was diluted in Krebs buffer (110 mM NaCl, 5.8 mM KCl, 25 mM $NaHCO_3$, 1.2 mM KH_2PO_4, 2.0 mM $CaCl_2$, 1.2 mM $MgSO_4$, and 11.1 mM glucose) just before use. Primary rabbit antibodies against EGFR and phosphorylated Y1173-EGFR (Cell Signaling Technology) were used at 1:1000 dilution. Rabbit polyclonal antibodies against ErbB2 and ErbB3 (Santa Cruz Biotechnology, Santa Cruz, CA) were used at 1:25 dilution. Mouse monoclonal antibody against phosphorylated (p)ERK (Santa Cruz Biotechnology) was used at 1:500 dilution. EGFR neutralizing antibody LA1 (Upstate Biotechnology, Lake Placid, NY) was used at 1 μg/ml. Ligand neutralizing antibodies against HB-EGF (R&D Systems, Minneapolis, MN), EGF (R&D Systems), and TGFα (Calbiochem) were used at 20 μg/ml.

Animals

Urinary bladders were obtained from female New Zealand White rabbits (3.5–4 kg; Myrtle's Rabbitry, Thompson Station, TN), female C57BL/6J mice (12–14 wk; The Jackson Laboratory, Bar Harbor, ME), and female Sprague-Dawley rats (250–300 g; Harlan, Indianapolis, IN). All animals were fed a standard diet with free access to water. Rabbits were euthanized by lethal injection of 300 mg of Nembutal into the ear vein, and mice and rats were euthanized by inhalation of 100% CO_2 gas and subsequent thoracotomy. All animal studies were approved by the University of Pittsburgh Animal Care and Use Committee.

Mounting of Uroepithelium in Ussing Stretch Chambers and Measurements of Tissue Pressure and Capacitance

Isolated uroepithelial tissue was dissected from underlying uroepithelium, which was then mounted on rings that exposed 2 cm^2 of tissue and mounted in an Ussing stretch chamber, as described previously (Wang *et al*., 2003). To simulate bladder filling, Krebs buffer was added to the mucosal hemichamber, filling it to capacity. The chamber was sealed, and an additional 0.5 ml of Krebs solution was infused, over a total of 2 min. Our initial reports described the pressure change induced by filling to be ~8 cm H_2O; however, new measurements using a more sensitive pressure transducer (TBM4 Transbridge pressure transducer; WPI, New Haven, CT) indicated that the final change in pressure was ~1 cm H_2O (Supplemental Figure S1). The pressure transducer was interfaced with a 1.8-GHz PowerPC G5 Macintosh computer (Apple, Cupertino, CA) and used Chart 5 software (ADInstruments, Castle Hill, Australia) for measurements. For slow filling, the mucosal chamber was filled at 0.1 ml/min using a NE-1600 pump (New Era Pump Systems, Farmingdale, NY); when the chamber was full, it was sealed and an additional 0.5 ml of Krebs' buffer was added at the same filling rate. The voltage response of the tissue to a square current pulse was measured and used to calculate the tissue's capacitance (where 1 μF = 1 cm^2 of apical membrane surface area) and monitor changes in the apical surface area of the umbrella cell layer of the uroepithelium (Wang *et al*., 2003). To unstretch the tissue, the sealed Luer ports were opened, and Krebs' buffer was rapidly removed from the apical chamber to restore baseline capacitance values. In some experiments, rabbit urine was collected from freshly excised bladders, centrifuged for 10 min at 10,000 $\times$ *g* at 4°C to remove precipitate and then added to the mucosal hemichamber.

Reverse Transcription-Polymerase Chain Reaction (RT-PCR) Analysis

Rabbit bladder tissue was isolated and pinned open on a rubber pad with the mucosal surface facing upwards. A 25-cm cell scraper (Sarstedt, Newton, NC) was used to scrape the uroepithelium, and scraped cells were collected into a 1.5-ml Eppendorf tube. The RNAqueous-4PCR kit (Ambion, Austin, TX) was used for lysis and total RNA preparation, as directed by the manufacturer. DNAse I treatment and DNAse inactivation were performed before reverse transcription, which was carried out according to instructions for RETROscript (Ambion) by using oligo(dT) primers. Amplification of ErbB family receptors and ligands was performed using standard PCR protocols and rabbit-specific sequence primer pairs as follows: target, 5'-primer 3'-primer; ErbB1, CAGCTACGAGGTGGAGGAAG GGATGTGCAGATCACCACTG; ErbB2, AAGTCCCGAGGACTGTCAGA GGACTCAAAGGTGTCCGTGT; ErbB3, GTCACATGGACACGATCGAC AAAGCAGTGGCCGTTACACT; ErbB4, GAACAATGTGATGGCAGGTG TTCGCATTGAAGTTGTGCTC; EGF, GAGGGAGGCTACACTTGCAT GGAGAGGGCTCATCTTCCTT; HB-EGF, GAGACCCATGTCTTCGGAAA CCACCACAGCCAGGATAGTT; and TGFα, AAGCCCTGGAGAACAG-CAC CAGAGTGGCAGACACATGCT.

Immunofluorescence and Image Acquisition

Rabbit, rat, and mouse bladders were isolated as described above. For FITC-EGF binding studies, tissue was incubated with 40 ng/ml FITC-EGF (Invitrogen) for 1 h at 4°C, and the tissue was washed with Krebs' buffer, three times for 5 min. In control experiments competing 400 ng/ml EGF was added 5 min before FITC-EGF addition. After incubation with ligand, the tissue was fixed, sectioned, stained, and imaged as described previously (Wang *et al*., 2005).

Activation of EGFR and Immunoblotting

After stretching rabbit uroepithelium in the Ussing stretch chamber for the indicated duration, the tissue was rapidly removed from the chamber and pinned, mucosal side up, to a rubber pad. The tissue was washed with ice-cold Krebs' solution and placed on ice. Next, 1 ml of lysis buffer (100 mM

NaCl, 50 mM tetraethylammonium, pH 8.6, 5 mM EDTA, 0.2% NaN_3, and 0.5% SDS) containing freshly added phosphatase inhibitor cocktail set II (Calbiochem), 0.5 mM phenylmethylsulfonyl fluoride, and 1 mM protease inhibitor cocktail was added to the bladder apical surface. The uroepithelium was scraped, and the cells were collected into a 1.5-ml Eppendorf tube. The scraped cells were sonicated (Sonic Dismembrator model 100; Fisher Scientific, Fair Lawn, NJ) on ice with 10 1-s pulses at a setting of 4. After centrifugation, the protein concentration of the lysate was determined using bicinchoninic acid assay reagents (Pierce Chemical, Rockford, IL). The samples were resolved by SDS-polyacrylamide gel electrophoresis (PAGE), transferred to nitrocellulose, and the membrane blocked overnight at 4°C with 5% nonfat milk in Tris-buffered saline + 0.05% Tween 20. After incubation with primary antibody, followed by horseradish peroxidase-conjugated anti-rabbit or anti-mouse antibodies, immunoreactive bands were visualized using SuperSignal West Substrate (Pierce Chemical) and exposed to Kodak BioMax MR Film (Eastman Kodak, Rochester, NY). Quantification was performed using Quantity One software (Bio-Rad, Hercules, CA).

Statistical Analysis

Statistically significant differences between means were determined by two-tailed Student's *t* test; $p < 0.05$ was considered statistically significant.

RESULTS

Tyrosine Phosphorylation Is Required for Stretch-induced Increases in Umbrella Cell Surface Area

In our experiments, isolated uroepithelium was mounted in a specialized Ussing stretch chamber and bladder filling was mimicked by increasing the hydrostatic pressure across the mucosal surface of the tissue (Wang *et al*., 2003) to a final pressure of ~1 cm H_2O (Supplemental Figure S1). Changes in mucosal surface area were monitored by calculating the transepithelial capacitance (where 1 μF $\cong$ 1 cm^2 of surface area), which primarily reflects changes in the apical surface area of umbrella cells and correlates well with other measures of apical exocytosis (Wang *et al*., 2003). In the absence of stretch or stimulation by pharmacological agents, there was no change in capacitance after 5 h (Figure 1A). However, when filling was performed over a period of 2 min the capacitance increased by ~50% after 5 h (Figure 1A).

The kinetics of the capacitance increase occurred in two phases: an "early phase," characterized by a rapid ~25% increase in surface area over the first 30 min; and a "late phase," in which the capacitance increased over a prolonged period that resulted in an additional ~25% increase during the next 4.5 h (Figure 1A). The late-phase increase in capacitance was eliminated by incubating the tissue for 60 min in cycloheximide before stretch, indicating that the late phase is dependent upon protein synthesis (Supplemental Figure S2). We previously showed that the secretory inhibitor BFA impaired release of newly synthesized secretory proteins from the apical pole of umbrella cells (Truschel *et al*., 2002). In this study, BFA treatment eliminated the late-phase increase, but it had no effect on the early-phase response to stretch (Figure 1B). This suggests that the early-phase response may depend on exocytosis of a preexisting pool of discoidal vesicles, whereas the late-phase response may be more dependent on the exocytosis of newly synthesized proteins. The increases in capacitance observed in response to stretch were rapidly reversed when pressure in the mucosal hemichamber was released after 30 min or 5 h of stretch (Figure 1C), and increased endocytosis was detected when FITC-labeled dextran or wheat germ agglutinin was included in the mucosal chamber during release (data not shown). The data in Figure 1C demonstrate that extended exposure to stretch does not affect the ability of the mucosal surface to recover from stretch. The stretch-induced changes in capacitance were largely independent of the rate of chamber filling, as confirmed by studies in which filling was performed at a rate of 0.1 ml/min, which raised the pressure to ~1 cm H_2O over 30 min (Supplemental Figure S3). Under these conditions the initial kinetics of capacitance change was somewhat slower, but the absolute change in capacitance was ~50% after 5 h. Because there was no discernible difference in the late-phase response, we used the rapid filling technique in subsequent studies to simplify our experiments.

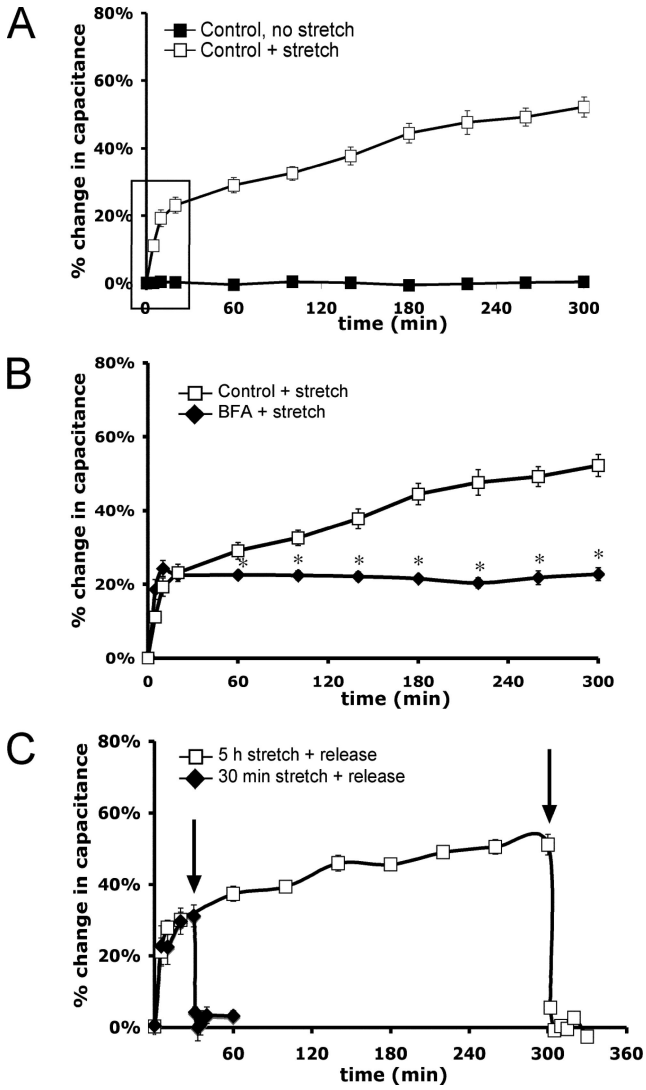

Figure 1. Characterization of the response to uroepithelial stretch. (A) Isolated rabbit uroepithelium was left unstretched or exposed to ~1 cm H_2O pressure (+ stretch) in an Ussing stretch chamber, and changes in membrane capacitance were measured. The box indicates the early phase increase in surface area upon stretch. (B) Tissue was pretreated with 5 μg/ml BFA for 10 min before stretching the tissue in the continued presence of BFA. *, Statistically significant difference ($p < 0.05$) relative to stretched samples. (C) Tissue was stretched for 30 min or 5 h and then the added Krebs' buffer was removed (indicated by arrows), releasing the stretch stimulus. Mean changes in capacitance ± SEM ($n \geq 3$) are shown.

Our studies focused on characterizing the signaling pathways involved in the late-phase, protein synthesis-dependent response to stretch. To examine whether tyrosine kinase signaling pathways were required for this response, the uroepithelium was stretched in the presence of 100 μM genistein, a broad-range inhibitor of tyrosine kinases and their signaling. Genistein treatment eliminated the late-

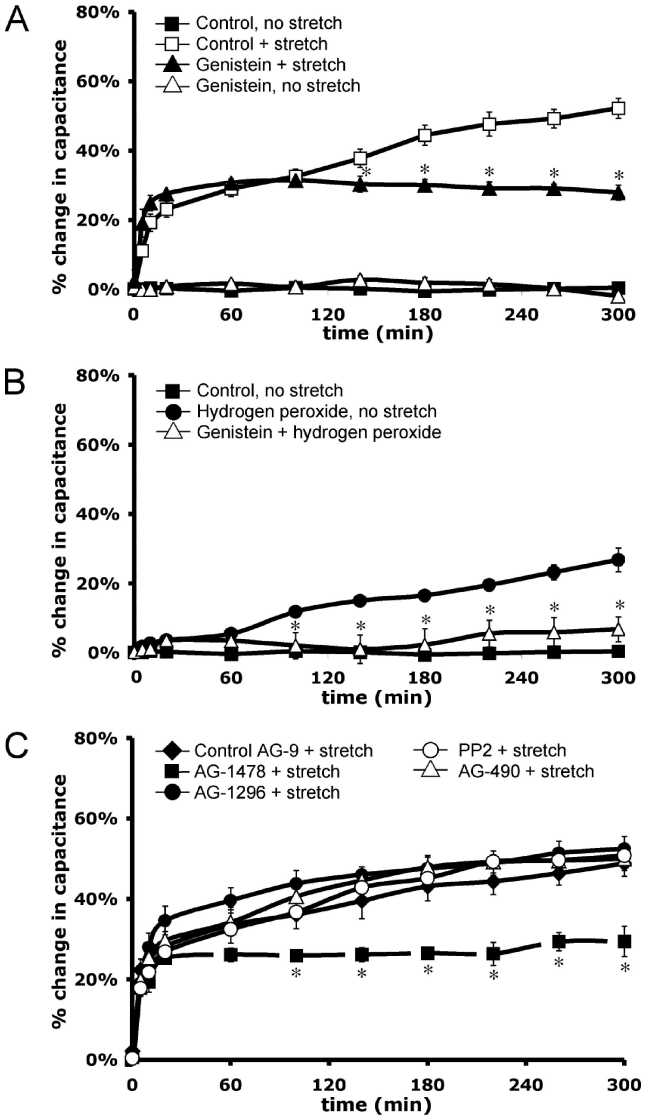

Figure 2. Tyrosine kinase signaling is required for the late-phase increase in capacitance. Rabbit uroepithelium was dissected and mounted in Ussing stretch chambers, equilibrated in the absence of pressure, and stretched at t = 0. (A) Genistein (100 μM) was added to both serosal and mucosal hemichambers for 30 min before stretch (genistein + stretch). As a control, the tissue received genistein treatment in the absence of stretch (genistein, no stretch). *, Statistically significant difference ($p < 0.05$) between genistein-treated and control stretched samples. (B) H_2O_2 was added to the mucosal chamber at t = 0 to a final concentration of 1 mM in the absence of stretch. Genistein treatment (as described above) was performed 30 min before H_2O_2 addition (genistein + hydrogen peroxide) and changes in capacitance were monitored. *, Statistically significant difference ($p < 0.05$) between treatment with H_2O_2 alone or treatment with H_2O_2 and genistein. (C) Both tissue surfaces were pretreated for 30 min with 25 nM AG-1478, 25 μM AG-1296, or 25 nM AG-9; or for 60 min with 30 μM AG-490 or 25 nM PP2; and then stretched in the continued presence of the drug. *, Statistically significant difference ($p < 0.05$) between AG-1478–treated and control stretch samples. Mean changes in capacitance ± SEM ($n \geq 3$) are shown.

phase increase in capacitance (Figure 2A). To further establish a role for tyrosine kinase signaling in regulating exocytosis in umbrella cells, nonstretched tissue was treated with hydrogen peroxide, which indirectly increases tyrosine phosphorylation by oxidizing a critical SH-group in the catalytic site of protein tyrosine phosphatases (Hecht and Zick, 1992). Hydrogen peroxide treatment induced an ~27% increase in surface area over 5 h. This response was significantly inhibited by pretreatment of the tissue with genistein (Figure 2B), indicating that the hydrogen peroxide-stimulated increase in capacitance was a likely consequence of increased tyrosine phosphorylation and not other nonspecific effects of hydrogen peroxide.

To explore which tyrosine kinase signaling pathways might be involved in modulating stretch-induced exocytosis, inhibitors were used that targeted tyrosine kinases implicated in mechanotransduction in other cell types, including the EGFR-selective antagonist tyrophostin AG-1478, the platelet-derived growth factor receptor inhibitor AG-1296, the Src-family selective inhibitor PP2, and the Janus tyrosine kinase (JAK)-2 inhibitor AG-490. Only treatment with AG-1478 significantly decreased the stretch-induced changes in the late-phase response (Figure 2C). The inactive tyrophostin AG-9 control had no significant effect on the stretch response (Figure 2C), and AG-1478 caused no changes in surface area in the absence of stretch (our unpublished data). AG-1478 similarly attenuated the stretch-induced capacitance changes in slowly stretched tissue (Supplemental Figure S3). Overall, the data indicated that stretch-induced changes in capacitance were dependent on tyrosine phosphorylation, most likely downstream of EGFR signaling.

ErbB Family Members and Their Ligands Are Expressed in the Uroepithelium

To determine the ErbB family receptor and ligand expression profile in the uroepithelium, total RNA from isolated rabbit uroepithelium was prepared, and message for rabbit ErbB family receptor and ligands was confirmed by RT-PCR. Rabbit nucleotide sequences for ErbB1–4, EGF, HB-EGF, and TGFα were obtained from the National Center for Biotechnology Information Center DNA sequence databases. Transcripts for EGFR, ErbB2, and ErbB3 were detected in all samples tested (n = 6), consistent with previous reports that showed ErbB1–3 expression in human uroepithelium (Rotterud *et al*., 2005). In contrast, ErbB4 transcript was not detected in five of six samples tested (Figure 3A), indicating that expression of ErbB4 was generally low or undetectable in this tissue. ErbB4 transcript was robustly detected in total RNA prepared from rabbit spinal cord, which was used as a positive control (our unpublished data). The mRNA for ErbB family ligands EGF, HB-EGF, and TGFα was present in all rabbit uroepithelial RNA preparations tested (Figure 3B), consistent with previous reports of these ligands being expressed in the uroepithelium (Mellon *et al*., 1996; Freeman *et al*., 1997). Negative control RT-PCR reactions using either scrambled primer pairs or no polymerase resulted in no PCR products (our unpublished data). The identities of the PCR products were verified by nucleotide sequencing.

Immunofluorescence staining was performed to confirm the expression of EGFR, ErbB2, and ErbB3 in the uroepithelium and to determine their distribution within this tissue. Bladder tissue was fixed, cryosectioned, and stained using ErbB receptor-specific antibodies, along with Topro-3 to label nuclei and rhodamine phalloidin to visualize the actin cytoskeleton. In mouse tissue, EGFR staining was observed in the cytoplasm of the underlying intermediate and basal cell layers as well as in the umbrella cell layer. In addition, EGFR was prominently localized near the apical surface of ~70% of umbrella cells (Figure 3C, left), whereas no staining was observed in the remaining 30% of umbrella cells. The reason for this disparity is unknown, but it may reflect

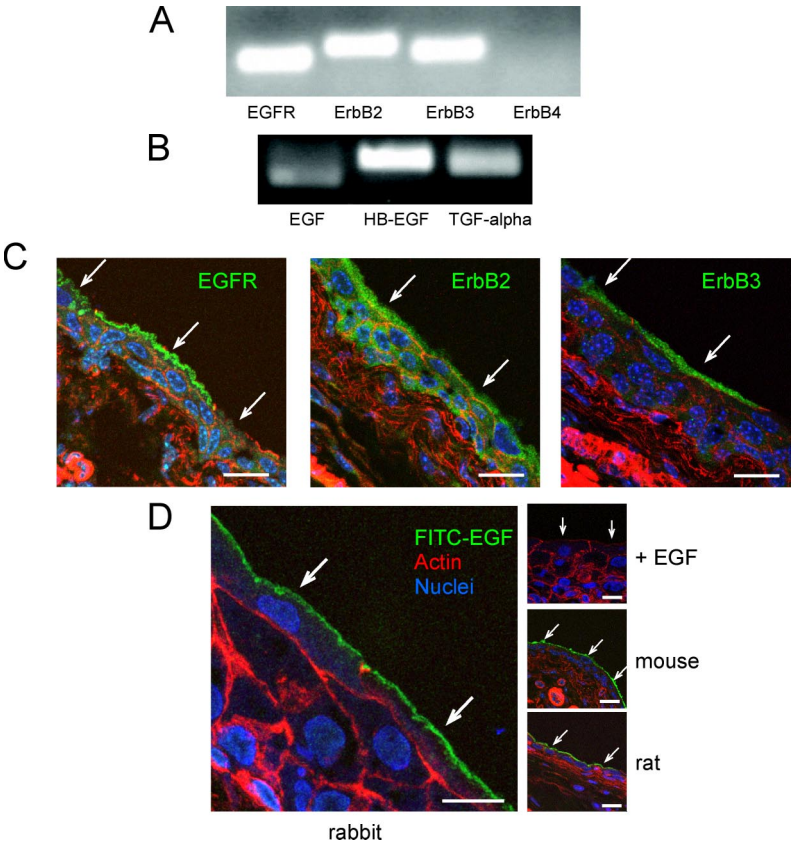

Figure 3. Expression and distribution of ErbB family receptors in the uroepithelium. (A and B) Total RNA was prepared from rabbit uroepithelium and RT-PCR used to assess expression of ErbB1–4 (A) or EGFR ligands EGF, HB-EGF, and TGFα (B). (C) Localization of ErbB family receptors in cryosections of mouse uroepithelium, labeled with antibodies to visualize the receptors (green), rhodamine-phalloidin to label the actin cytoskeleton (red), and Topro-3 to label nuclei (blue). Bar, 20 μm. (D) Binding of FITC-EGF to rabbit uroepithelium (far left), in which tissue was bathed in 40 ng/ml FITC-EGF at 4°C for 1 h, washed, fixed, and sectioned. In the control study (right, top), FITC-EGF binding to rabbit tissue was competed with excess unlabeled EGF (400 ng/ml). FITC-EGF binding to the apical surface of mouse and rat umbrella cells is shown in the right middle and right bottom panel, respectively. Bar, 15 μm for rabbit tissues and 20 μm for mouse and rat tissues. Individual umbrella cells are indicated by arrows.

differences in the state of umbrella cell differentiation or their state of response to bladder filling/voiding. A similar EGFR staining pattern was observed in rabbit bladder tissue (our unpublished data). Immunofluorescence studies of mouse bladder tissue revealed ErbB2 staining throughout all layers of the uroepithelium (Figure 3C, middle) and ErbB3 staining within the umbrella cell layer of the uroepithelium (Figure 3C, right).

To confirm that EGFR was present at the apical surface of umbrella cells, rabbit bladder tissue was incubated with 40 ng/ml FITC-EGF for 1 h at 4°C, washed, fixed, and sectioned. Although FITC-EGF was added to both the serosal and mucosal surfaces of the tissue, appreciable binding was observed only at the apical surface of rabbit umbrella cells (Figure 3D, far left). As a control, the tissue was incubated with competing unlabeled 400 ng/ml EGF, which effectively eliminated FITC-EGF staining (Figure 3D, right top). Binding of FITC-EGF to the apical surface of umbrella cells was also observed in mouse and rat uroepithelium (Figure 3D, right middle and bottom, respectively), further establishing the presence of EGFR on the mucosal surface of umbrella cells. In summary, the aforementioned data confirmed expression of ErbB family receptors and ligands, including EGFR, EGF, HB-EGF, and TGFα in the uroepithelium. Furthermore, the data indicated that EGF binds to the apical surface of the umbrella cell layer, where it may stimulate EGFR-dependent signaling.

EGF Stimulates Exocytosis in the Uroepithelium

To determine whether EGFR signaling induced membrane turnover in the uroepithelium, we explored the effects of adding EGF to either the mucosal or serosal surface of the tissue. The addition of 100 ng/ml EGF to the apical surface of the uroepithelium caused an ~31% increase in surface area over 5 h (Figure 4A). A similar increase (~34%) was observed upon addition of 100 ng/ml EGF to the serosal surface (Figure 4A). Interestingly, the kinetics of the response to EGF addition was reminiscent of the late-phase increase in response to stretch; a gradual increase of ~30% over 5 h. A similar response (~30% increase) was observed upon addition of other ErbB family ligands in the absence of stretch, including 100 ng/ml HB-EGF, 25 ng/ml TGFα, and 100 ng/ml heregulin-β (our unpublished data). The effect of simultaneous addition of EGF to both surfaces was not additive, indicating that the signaling mechanisms from either surface were likely to be similar, if not identical. When EGF at 100 ng/ml was added at the same time as stretch, the overall increase was not significantly different from stretch alone (our unpublished data), demonstrating that the signaling pathways for these two stimuli were also not additive. The specificity of the EGF response was confirmed by preincubation of the tissue with AG-1478 (Figure 4A) or treatment with BFA (Figure 4B), both of which significantly inhibited EGF-dependent responses. We also examined whether the EGF-stimulated increases in capacitance required chronic treatment with ligand or whether a short pulse of EGF was sufficient to stimulate exocytosis. A 5-min treatment of EGF, followed by washes to remove the added EGF, was sufficient to stimulate an ~20% increase in capacitance (Figure 4C).

There is an appreciable amount of EGF and other EGFR ligands present in urine (Fisher *et al.*, 1989; Keay *et al.*, 2000). To determine whether these urinary ligands were able to stimulate discoidal vesicle exocytosis, we added undiluted urine to the mucosal chamber of unstretched tissue and monitored capacitance. However, we found that addition of

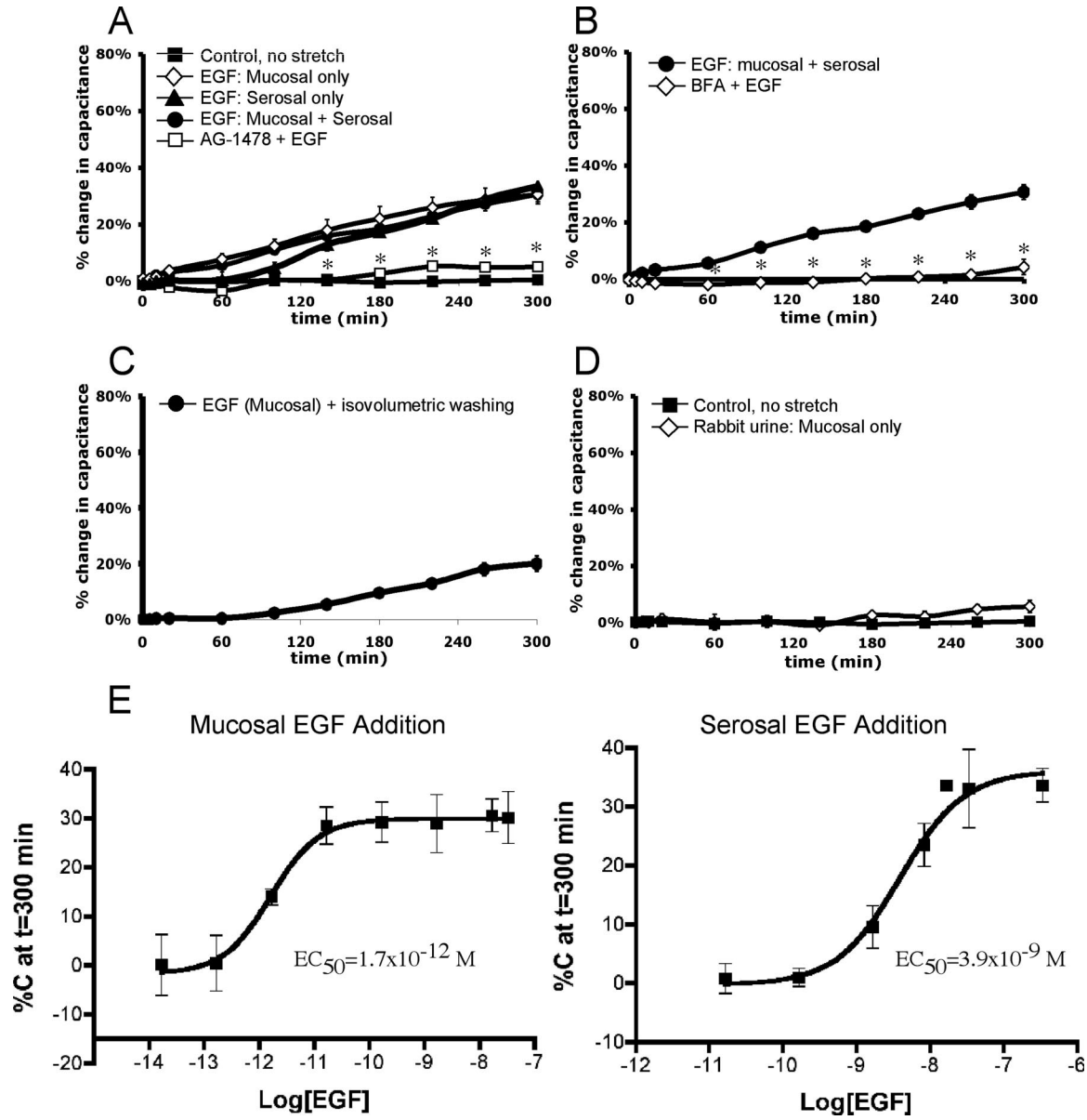

Figure 4. Exogenous EGF stimulates capacitance increases in the absence of stretch. Rabbit uroepithelium was mounted in Ussing stretch chambers and incubated in the absence of pressure. (A) Changes in capacitance were recorded upon addition of 100 ng/ml EGF (±30-min pretreatment with AG-1478) to the serosal, mucosal, or both surfaces. (B) Tissue was pretreated with 5 μg/ml BFA before addition of 100 ng/ml EGF to both surfaces of the uroepithelium (BFA + EGF). (C) EGF was added to the mucosal hemichamber, and after 5 min the buffer in the mucosal hemichamber was replaced with buffer lacking EGF. The change in capacitance was recorded. (D) Effect of undiluted rabbit urine on capacitance changes. (E) Dose–response curves for the change in capacitance recorded 5 h after addition of EGF to mucosal or serosal surface of the uroepithelium. In each panel, the mean changes in capacitance ± SEM ($n \geq 3$) are shown. *, In A and B, statistically significant difference ($p < 0.05$) relative to addition of EGF to both surfaces.

urine caused no significant change in capacitance over 5 h (Figure 4D).

Dose–response studies were performed to determine the EC_{50} value for EGF-induced changes in capacitance. The EC_{50} value for mucosally added EGF was 1.7×10^{-12} M, which was ~2000-fold more potent than the EC_{50} value for serosally added EGF (3.9×10^{-9} M) (Figure 4E). In subsequent studies, we used the minimum effective concentration of EGF that induced an ~30% increase in stretch: 0.1 ng/ml EGF mucosally and 100 ng/ml EGF serosally. In summary, addition of EGF (as well as other ErbB-family ligands) to either surface of the bladder tissue stimulated an increase in mucosal surface area in the absence of stretch, although EGF treatment was significantly more potent when added to the mucosal surface of the tissue.

Stretch Stimulates Autocrine Activation of EGFR by HB-EGF

Because EGFR signaling appeared to be necessary for late-phase, stretch-induced changes in capacitance, EGFR activation was assessed by examining the phosphorylation state of Y_{1068} and Y_{1173}, residues that are autophosphorylated in

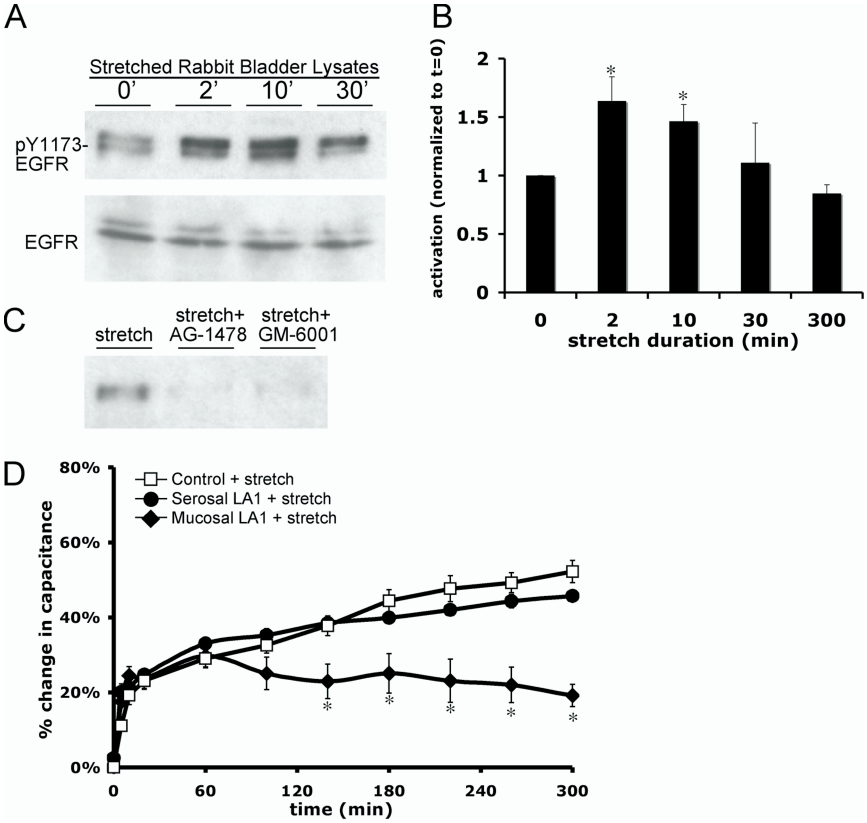

Figure 5. Stretch activates the EGFR. (A) Tissue was stretched for the indicated time, lysates of rabbit uroepithelium were prepared and resolved by SDS-PAGE, and Western blots were probed with antibodies specific for phosphorylated Y_{1173}-EGFR or total EGFR. (B) Quantification of Y_{1173} phosphorylation in response to stretch, relative to unstretched (t = 0') tissue samples. The mean changes in capacitance ± SEM are shown (n = 4). *, Statistically significant difference ($p < 0.05$) relative to unstretched tissue. (C) Tissue was stretched for 2 min in the absence of additional treatment, or pretreated for 30 min with 25 nM AG-1478 or 10 μM GM-6001 before stretch, followed by lysate preparation. (D) Rabbit uroepithelium was placed on tissue rings and the mucosal or serosal surfaces were pretreated with 1 μg/ml LA1 EGFR function-blocking antibody for 1 h before mounting, equilibrating, and stretching the tissue in Ussing stretch chambers. The mean changes in capacitance ± SEM ($n \geq 3$) are shown. *, Statistically significant difference ($p < 0.05$) relative to control stretch samples.

response to receptor activation (e.g., upon ligand binding, Helin *et al.*, 1991). In our experiments, the uroepithelium was stretched in Ussing stretch chambers for up to 5 h, and then the tissue was rapidly removed from the chamber, placed on ice, scraped, and lysed (the isolation of tissue and preparation of lysate took ~5 min to complete). Total and phosphorylated EGFR were detected in lysates by Western blot. Stretch was accompanied by a significant increase in Y_{1173}–EGFR phosphorylation that was apparent in as little as 2 min, and EGFR phosphorylation remained elevated for at least 10 min after stretch, but it returned to baseline over time (Figure 5, A and B). Similar results were observed using an antibody specific for Y_{1068} phosphorylation (our unpublished data). As predicted, treatment with AG-1478 attenuated receptor phosphorylation (Figure 5C).

To ascertain the side of the tissue from which EGFR signaling occurred during stretch, a function-blocking EGFR antibody (LA1) was added to the mucosal or serosal surface of stretched tissue. Addition of the antibody to the mucosal surface blocked the late-phase capacitance change (Figure 5D). Conversely, addition of the antibody to the serosal surface of the tissue had no significant effect on capacitance changes (Figure 5D). Because the serosal surface of our epithelial preparation contains residual connective, nervous, and muscle tissue that may impair access of large molecules such as antibodies, we cannot rule out a role for basolateral EGFR in this process. However, the ability of mucosal LA1 and ligand-specific antibodies (see below) to completely block the late-phase increase in capacitance indicates that events at the apical surface of the umbrella cell are those most likely to be physiologically relevant to changes in mucosal surface area.

EGFR can be activated in an autocrine, paracrine, or juxtacrine manner (Singh and Harris, 2005). Autocrine activation is modulated by metalloproteinases, which proteolytically cleave the transmembrane precursors of the ligands, releasing soluble ligands that can then bind and initiate receptor activation (Singh and Harris, 2005). To explore the mechanism of ligand production in our system, uroepithelial tissue was treated with GM-6001, a broad-spectrum metalloproteinase inhibitor. Treatment with GM-6001 blocked stretch-activated EGFR phosphorylation (Figure 5C) and reduced the late-phase tissue response to stretch (Figure 6A). In contrast, the catalytically inactive GM-6001 (negative control) treatment had no effect on the response (Figure 6A). To define which ligand may be responsible for receptor activation, function-blocking antibodies to EGF, HB-EGF, or TGFα were added to the mucosal surface of the tissue for 1 h before tissue equilibration in the Ussing chamber. Mucosal addition of HB-EGF neutralizing antibody attenuated the late-phase capacitance response, whereas addition of antibodies to TGFα or EGF had no significant effect on the response (Figure 6B).

As further evidence that autocrine activation of EGFR was due to HB-EGF binding, the mucosal surface of the tissue was incubated with 5 μg/ml CRM-197, a nontoxic variant of *Corynebacterium* diphtheria toxin that strongly binds to membrane-associated and soluble HB-EGF, preventing HB-EGF from activating EGFR (Mitamura *et al.*, 1995). CRM-197 binding does not affect the activity of other ErbB ligands. CRM-197 treatment significantly inhibited the late-phase, stretch-induced changes in capacitance, and this effect was partially rescued by the simultaneous addition of EGF (100 ng/ml) to the mucosal hemichamber (Figure 6C). Together, the aforementioned studies indicate that EGFR is activated by stretch and that stretch-induced capacitance changes are initiated at the

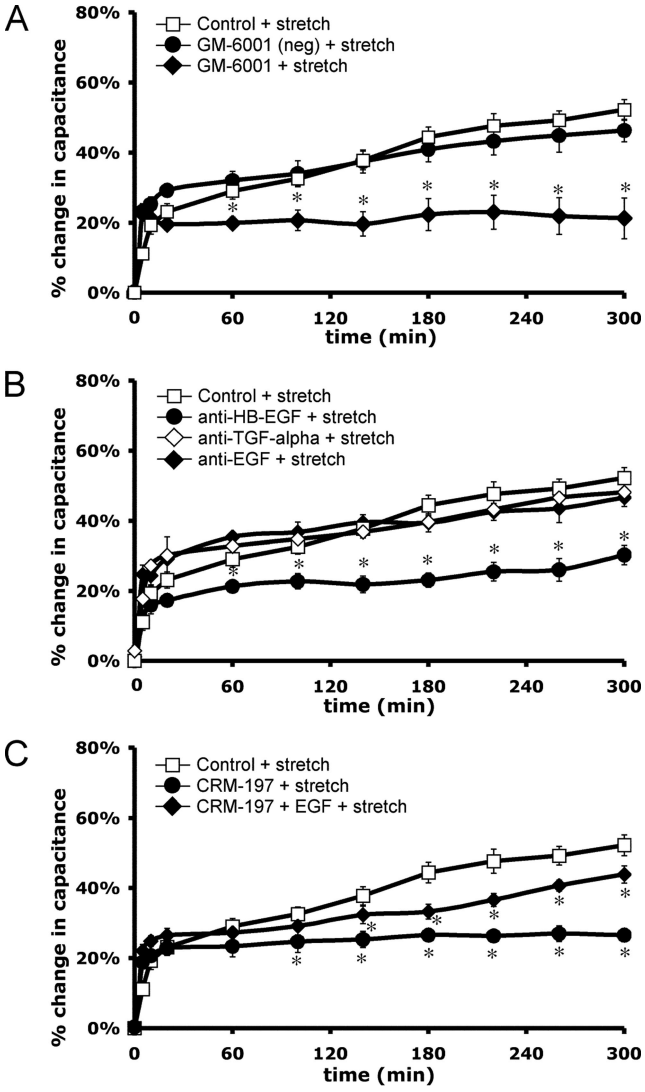

Figure 6. Metalloproteinase activity and HB-EGF ligand are required for stretch-induced capacitance changes. Rabbit uroepithelium was isolated and mounted in Ussing stretch chambers. (A) Tissue was pretreated with 10 μM GM-6001 or inactive GM-6001 analogue for 30 min before stretch. (B) Tissue was incubated with the specified ligand-neutralizing antibodies (20 μg/ml) added to the mucosal surface for 1 h before equilibration of the tissue and stretch. (C) Tissue was pretreated 30 min with 5 μg/ml CRM-197 toxin and then stretched in the presence or absence of 100 ng/ml mucosal EGF. In each panel, mean changes in capacitance $\pm$ SEM ($n \geq 3$) are shown. *, Statistically significant difference ($p < 0.05$) relative to control stretch samples.

mucosal surface of the tissue as a result of autocrine activation of receptor upon HB-EGF binding.

EGFR-stimulated Exocytosis Depends on Protein Synthesis and Acts via MAPK Signaling

The late-phase changes in capacitance are dependent on protein synthesis (Supplemental Figure S2). However, the upstream mechanism that initiates this synthesis is unknown. The EGFR can regulate protein synthesis through several mechanisms, including downstream stimulation of MAPK cascades. In the classical MAPK pathway, extracellular stimuli lead to the activation of MAPKs through the serial phosphorylation of a cascade of serine/threonine-specific protein kinases, including the MAPK kinase kinase (e.g., Raf); the MAPK kinase (e.g., MEK1/2); and finally the target MAPK, such as p38, JNK, or ERK1/2. The phosphorylated MAPK, in turn, phosphorylates transcription factors that alter gene expression (Pearson *et al.*, 2001). Although EGFR signaling activates many downstream signaling pathways, including phosphoinositide 3-kinase, JAK-signal transducer and activator of transcription (STAT), and protein kinase C, we chose to focus on MAPK signaling because of its known interface with protein synthesis regulation machinery and our interest in the late-phase response to stretch.

To further dissect the pathway by which EGFR signaling induces the late-phase increase in surface area, we examined whether the EGF-dependent increase in capacitance required protein synthesis. Indeed, when uroepithelial tissue was pretreated with 100 μg/ml cycloheximide for 1 h, the response to EGF was eliminated (Figure 7A). Next, we examined whether MEK1/2, the upstream kinase that activates ERK1/2, was involved in the response to stretch. The MEK1 inhibitor PD-098059 (10 μM) and dual MEK1/2 inhibitor U0126 (10 μM) both caused a significant attenuation of the stretch-induced capacitance response, effectively eliminating the late-phase rise in capacitance (Figure 7B). These inhibitors were also effective in eliminating EGF-induced increases in surface area (Figure 7C). Treatment with SB-203580 (10 μM), a p38 MAPK-selective inhibitor, also attenuated the late-phase, stretch-induced increase in surface area (Figure 7B), and it eliminated the capacitance increase in response to EGF (Figure 7C). In contrast, the JNK Inhibitor II (500 nM) had no significant effect on stretch- or EGF-induced capacitance changes (Figure 7, B and C).

Finally, we examined whether ERK1/2 was phosphorylated as a result of stretch and whether its activation occurred downstream of EGFR activation. When Western blots of lysates (obtained from tissue $\pm$ stretch) were probed with antibodies that detect phosphorylated forms of ERK1/2, stretch stimulated the phosphorylation of ERK1/2 (Figure 7D). Stretch-stimulated phosphorylation of ERK1/2 was attenuated by treatment with either AG-1478 or GM-6001 (Figure 7E), indicating that the ERK1/2 phosphorylation was dependent on upstream EGFR activation. Collectively, these studies implicate MAPK signaling cascades as acting downstream of EGFR activation to stimulate stretch-induced changes in capacitance, possibly by regulating changes in protein synthesis.

DISCUSSION

Mechanotransduction is a complex process that converts physical stimuli into biological responses. Although stretch-activated channels, integrins, and intracellular signaling pathways such as tyrosine kinase signaling cascades have been implicated in these responses, we still lack a precise understanding about how mechanical inputs are sensed and deciphered by the cell (Apodaca, 2002; Huang *et al.*, 2004). Previous analysis has pointed to roles for the EGFR and ErbB family members in bladder development, hypertrophy of bladder smooth muscle in response to mechanical stress, and pathogenesis of transitional cell carcinoma (Baskin *et al.*, 1996; Nguyen *et al.*, 2000; Cheng *et al.*, 2002). Other than studies showing potential roles for ErbB signaling in the regulation of uroepithelial growth and proliferation (Baskin *et al.*, 1996; Bindels *et al.*, 2002), significantly less information is available about the physiological function of EGFR in the uroepithelium. Our data provide a novel link between me-

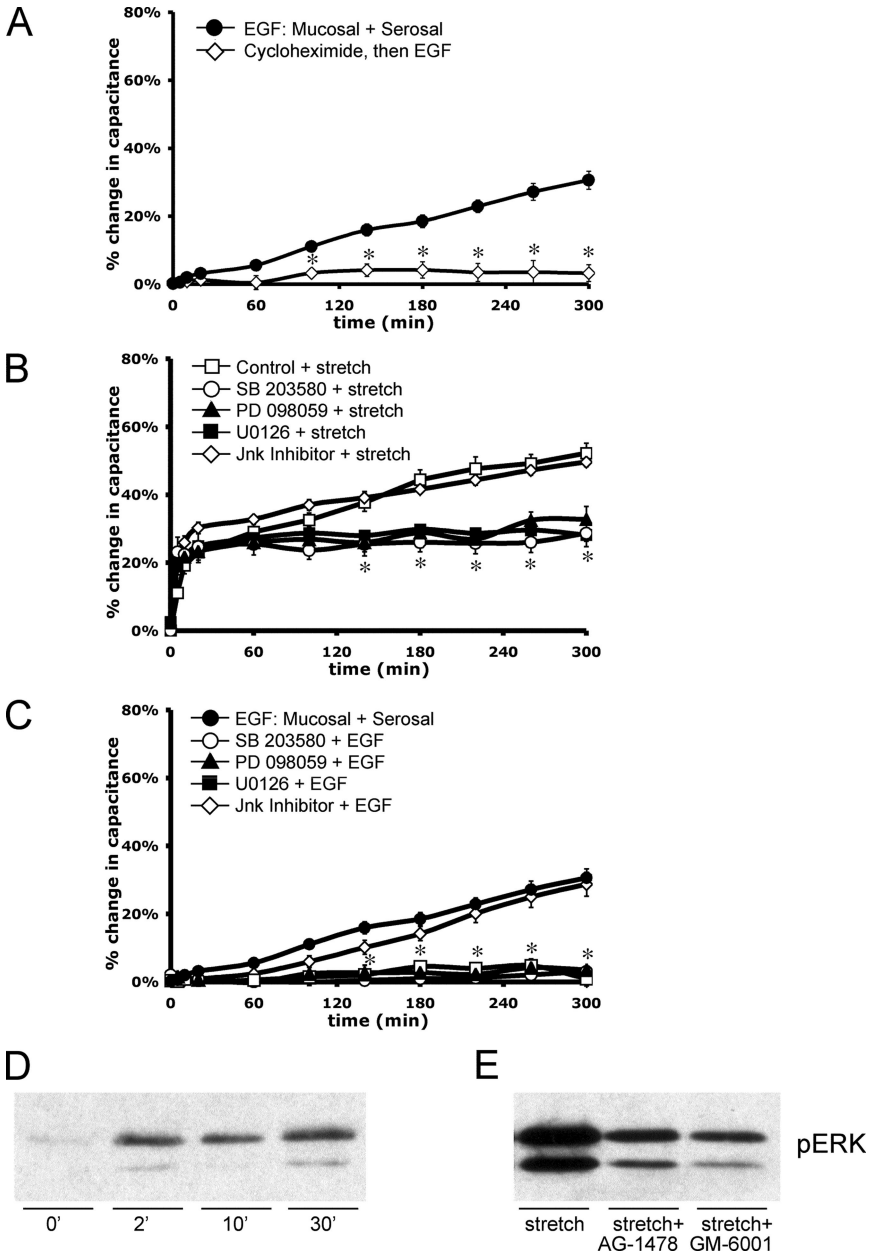

Figure 7. Protein synthesis and MAPK signaling pathways are required for EGF- and stretch-induced late-phase capacitance increases. Rabbit uroepithelium was isolated and mounted in Ussing stretch chambers. (A) Tissue was incubated with 100 ng/ml EGF (±60-min pretreatment with 100 μg/ml cycloheximide). *, Statistically significant difference ($p < 0.05$) relative to EGF-treated samples. (B) Before stretch, tissue was pretreated with p38 inhibitor SB-203580 (10 μM for 1 h), MEK1 inhibitor PD-098059 (10 μM for 30 min), MEK1/2 inhibitor U0126 (10 μM for 30 min), or JNK inhibitor II (500 nM for 30 min) as indicated. *, Statistically significant differences ($p < 0.05$) relative to control samples were observed for tissue treated with SB-203580, PD-098059, or U0126 at $t \geq 140$ min. (C) Before treatment with 100 ng/ml EGF, tissue was incubated with SB-203580, PD-098059, U0126, or JNK inhibitor II as described above. *, Statistically significant differences ($p < 0.05$) relative to control samples were observed for tissue treated with SB-203580, PD-098059, or U0126 at $t \geq 100$ min. In each panel, the mean changes in capacitance ± SEM ($n \geq 3$) are shown. (D) Tissue was stretched for the indicated time before lysate preparation. Western blots were probed with antibodies specific for pERK1/2. (E) Tissue was left untreated (stretch) or pretreated for 30 min with 25 nM AG-1478 (AG) or 10 μM GM-6001 (GM) as indicated. Tissue was then stretched for 2 min before lysate preparation and blotting with phospho-specific antibodies to ERK1/2.

chanical stimuli, apical EGFR signaling, and changes in apical membrane turnover in the umbrella cell layer of the uroepithelium.

Distribution of ErbB Family Receptors in Epithelia, Including the Uroepithelium

In the mammalian bladder, the EGFR and other ErbB family members have been variably localized in the uroepithelium (Messing, 1990; Chow *et al*., 1997; Rotterud *et al*., 2005), with the majority of studies reporting that the EGFR is found in the basal cell layers. EGFR is typically localized to the basolateral surface of polarized cells. In contrast, our data indicate that the EGFR is localized, in part, to the apical surface of the umbrella cell layer where, as discussed below, it regulates apical membrane turnover. Data in support of the apical localization of EGFR included 1) our immunofluorescence studies showing that the EGFR in both mice and rabbits was localized at or near the apical surface of the umbrella cell layer; 2) demonstration that FITC-labeled EGF bound to the apical surface of umbrella cells at 4°C in rabbit, rat, and mouse tissue; 3) the ability of small amounts of apically administered EGF to stimulate exocytosis (with an EC_{50} value of ~2 pM); and 4) the finding that neutralizing anti-EGFR–specific antibodies or anti-HB-EGF antibodies impaired stretch-induced exocytosis when added to the mucosal surface of the isolated uroepithelium.

Activation of EGFR by Uroepithelial Stretch: A Possible Autocrine Loop

The EGFR is activated by mechanical stimuli in a number of cell types, including mesangial cells, keratinocytes, vascular smooth muscle cells, type II alveolar cells, bronchial epithelial cells, cardiac myocytes, and proximal tubule cells (Kudoh *et al*., 1998; Iwasaki *et al*., 2000; Alexander *et al*., 2004;

Sanchez-Esteban *et al*., 2004; Tschumperlin *et al*., 2004; Yano *et al*., 2004; Krepinsky *et al*., 2005). However, the link between mechanical stimuli, EGFR activation, and changes in membrane traffic has not been described. We observed that stretching the uroepithelium stimulated a rapid increase in EGFR receptor phosphorylation, and treatments that blocked EGFR activation (e.g., treatment with AG-1478 or apical addition of LA1 anti-EGFR antibody) inhibited late-phase changes in exocytosis.

Although these data indicate that EGFR signaling initiated at the apical surface of the umbrella cells is primarily responsible for the late-phase stretch-induced changes in surface area, we cannot rule out a role for EGFR at the serosal surface of the tissue. Moreover, EGF (in the absence of stretch) stimulated similar changes in capacitance when added to either surface of the tissue; however, mucosal EGF was ~2000-fold more potent at stimulating exocytosis than serosal EGF. The EC_{50} for EGF-stimulated changes in apical membrane capacitance (~2.0 pM) was similar to the reported 10–100 pM K_D associated with the high-affinity type EGFR (Lax *et al*., 1989), indicating that subnanomolar amounts of ligand are sufficient to give the maximal response. The EGFR can form homodimers or heterodimers with ErbB2–4, and because ErbB2 and ErbB3 were expressed in the uroepithelium, it is possible that other ErbB family receptors are activated during stretch-induced changes in exocytosis by formation of heterodimers with EGFR. The higher EC_{50} value we measured upon serosal EGF addition may suggest the presence of lower affinity receptors present at the basolateral surface of the umbrella cells. However, this interpretation is likely to be simplistic, because there are multiple cell types present on the serosal side of the tissue, and we cannot rule out that EGF is binding to underlying cell types that release secretagogues that stimulate exocytosis in the umbrella cell layer. As such, the higher EC_{50} value could reflect mixed populations of low- and high-affinity EGFRs present on different cell types, decreased receptor density, or increased turnover of ligand or receptors at this surface of the tissue.

EGFR activation in our system is likely via an autocrine mechanism. Consistent with previous studies (Mellon *et al*., 1996; Freeman *et al*., 1997), we observed that rabbit uroepithelium expressed the ErbB ligands EGF, HB-EGF, and TGFα. Importantly, we observed that addition of function-blocking antibodies directed against HB-EGF, but not EGF or TGFα, inhibited late-phase changes in exocytosis when added to the mucosal surface of the tissue. Furthermore, we observed that the general metalloproteinase inhibitor GM-6001 inhibited stretch-induced EGFR activation and blocked late-phase changes in exocytosis, consistent with blocking the generation of HB-EGF. However, we cannot rule out that GM-6001 blocked exocytosis by preventing metalloproteinase-dependent cleavage of an unknown substrate required for stretch-regulated exocytosis.

Autocrine activation of EGFR by mechanical stimuli such as stretch may occur as a result of receptor transactivation, where an upstream stimulus such as elevated intracellular Ca^{2+}, exposure to radiation, or activation of G protein-coupled receptors promotes proteolytic processing and release of ErbB family ligands, typically HB-EGF, that rapidly bind to and activate the EGFR (Daub *et al*., 1996). We previously reported that stretch stimulates rapid release of ATP from the uroepithelium, and that serosal ATP acts through a Ca^{2+}-dependent pathway to stimulate umbrella cell discoidal vesicle trafficking (Wang *et al*., 2005). However, our previous studies could not rule out a role for G protein-coupled P2Y receptors in this process.

One plausible model is that ATP binds to P2Y receptors, which in turn stimulates a heterotrimeric G protein to activate proteolytic cleavage and release of ligand(s) such as HB-EGF. Transactivation of EGFR downstream of ATP has previously been shown to occur in Muller glial cells (Milenkovic *et al*., 2003). Alternatively, the increased Ca^{2+} stimulated by ATP binding to P2X receptors could result in EGFR transactivation. The extremely low EC_{50} value we measured for EGF-stimulated increases in exocytosis indicates that even small amounts of local ligand production would be sufficient to stimulate exocytosis. It is equally plausible that many of the mediators we have previously found to stimulate exocytosis, such as adenosine and agents that increase intracellular Ca^{2+} and cAMP (Truschel *et al*., 2002; Wang *et al*., 2003, 2005; Yu *et al*., 2006), may act, in part, by EGFR transactivation.

We examined the possibility that EGFR ligands present in urine may activate the EGFR in a paracrine manner. However, we found that urine added to the mucosal surface of

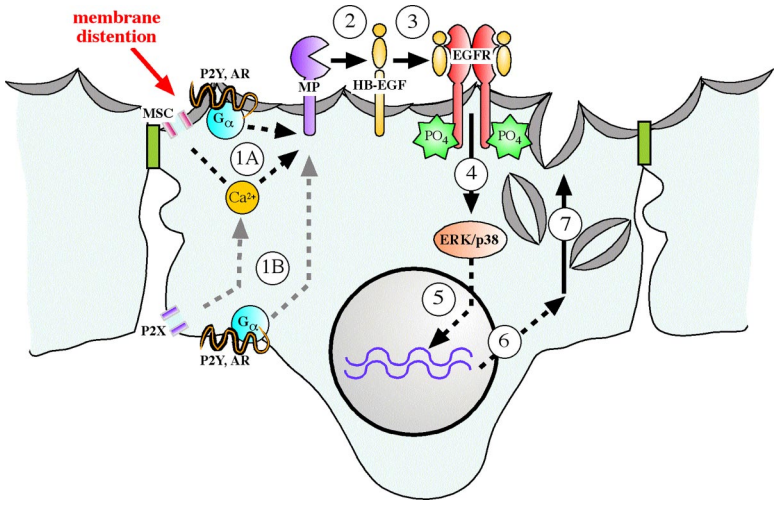

Figure 8. Model for regulation of late-phase exocytosis by transactivation of EGFR and downstream MAPK-dependent protein synthesis. The mechanical distention caused by bladder filling may stimulate release of mediators such as ATP and adenosine (not shown in figure) (Wang *et al*., 2005; Yu *et al*., 2006), which bind to P2X, P2Y, or adenosine receptors (AR). Alternatively, filling may directly activate other signaling pathways such as those initiated by putative mechanosensitive channels (MSC). The increased intracellular Ca^{2+} or activation of heterotrimeric G proteins that initiates at the mucosal (step 1A) or possibly serosal (step 1B) surfaces of the cell activates metalloproteinase activity through an uncharacterized mechanism. The metalloproteinase (possibly a member of the a disintegrin and metalloproteinase family or matrix-associated metalloproteinase family) cleaves apical pro-HB-EGF (step 2) to liberate soluble HB-EGF, which stimulates EGFR dimerization and cytoplasmic auto-phosphorylation (step 3), allowing recruitment of signaling molecules including those that may activate p38 and ERK1/2 MAPK signaling pathways (step 4). MAPK signaling pathways may regulate the transcription of gene products (step 5), which encode unknown proteins (step 6) that facilitate exocytosis of discoidal vesicles that mediate the late-phase expansion of apical surface area (step 7).

the isolated uroepithelium did not stimulate exocytosis. This may indicate that urinary EGFR ligands may not be functional, e.g., urinary exopeptidases and endopeptidases could decrease the fraction of active EGF (Mount *et al*., 1985; Fisher *et al*., 1989), or they may have limited access to EGFR present on the apical surface of the umbrella cells. However, we cannot rule out a paracrine role for EGF at the serosal surface of the tissue as EGF addition at this surface of the tissue stimulated exocytosis in the umbrella cell layer.

We also observed that exogenous stimulation of the EGFR by EGF addition caused a slow rise in capacitance, similar to the late-phase increase in response to stretch; however, this response was not reversible upon EGF washout. In contrast, stretch-induced changes in capacitance were fully reversible, indicating that "unstretching" the tissue activated its own set of responses that effectively turned off the pathway(s) that stimulated exocytosis. These unstretching responses are likely to include increased compensatory endocytosis of apical membrane in a pathway independent of EGFR signaling. Future studies will explore the uroepithelial response to removal of a stretch stimulus and the endocytic pathways associated with bladder voiding.

Requirement for MAPK Signaling and Protein Synthesis

The early phase of the stretch-induced capacitance increase is inhibited by the P2 receptor antagonist pyridoxal-phosphate-6-azophenyl-2′,4′-disulfonic acid and agents that deplete extracellular ATP (Wang *et al*., 2005), and it is insensitive to cycloheximide treatment (Truschel *et al*., 2002; Supplemental Figure S2). In contrast, the late-phase capacitance response is dependent on protein synthesis (Supplemental Figure S2). Although we do not know the nature or identity of the proteins whose synthesis is altered in response to stretch, our data indicate that their expression may be altered downstream of MEK1/2 and possibly p38 MAPK signaling pathways. In contrast, a JNK-selective inhibitor had no effect on the stretch- or EGF-induced response. The likely requirement for both MEK/ERK and p38 indicates that they may regulate distinct classes of gene products, both of which are required for late-phase increases in capacitance. The activation of other ErbB downstream pathways (such as phosphoinositide 3-kinase, JAK-STAT, and protein kinase C) and their roles in stretch-induced trafficking in the bladder have not been explored, but they may also have significance in uroepithelial biology.

Concluding Remarks

The apical plasma membrane of epithelial cells serves as a signaling platform that receives input from the extracellular milieu. Through surface receptors and channels and their associated signaling cascades, extracellular stimuli are transduced into changes in cell function. In the umbrella cell, exocytosis/endocytosis at the apical surface of the cell is particularly important, because it allows for surface area expansion during bladder filling (and recovery of membrane upon voiding), and modulation of the sensory input/output pathways by regulating the release of transmitters and the density of receptors at the surface of the umbrella cell. This regulation is likely to be clinically important, because increased ErbB family receptor expression is observed in bladder cancers (Messing, 1990; Chow *et al*., 1997; Rotterud *et al*., 2005), and painful bladder conditions are associated with increased ATP release and expression of increased levels of nociceptive $P2X_2$ and $P2X_3$ receptor subunits (Sun *et al*., 2001; Birder *et al*., 2004). In this report, we provide evidence that bladder filling may stimulate autocrine activation of EGFR at the apical pole of the umbrella cell layer, initiating a signaling cascade that regulates the extended late phase of exocytosis in the umbrella cell layer in a MAPK- and protein synthesis-dependent manner (Figure 8). The uroepithelium is thus an excellent model system to explore the interface between the apical membrane of epithelial cells, mechanical stimuli, growth factor signaling, and apical membrane dynamics. Furthermore, these data offer a novel function for apical EGFR in the regulation of surface area changes in the uroepithelium during physiological stretch.

ACKNOWLEDGMENTS

We kindly thank Drs. Rebecca Hughey, Ora Weisz, and Matthew Hawryluk for invaluable input during manuscript preparation. This work was supported by grants from the National Institutes of Health to E.M.B. (National Institute of Biomedical Imaging and Bioengineering, F31-EB0051450) and G.A. (National Institute of Diabetes and Digestive and Kidney Diseases, R37-DK54425).

REFERENCES

Alberts, B. (2002). Molecular Biology of the Cell, New York: Garland Science.

Alexander, L. D., Alagarsamy, S., and Douglas, J. G. (2004). Cyclic stretch-induced cPLA2 mediates ERK 1/2 signaling in rabbit proximal tubule cells. Kidney Int. *65*, 551–563.

Apodaca, G. (2002). Modulation of membrane traffic by mechanical stimuli. Am. J. Physiol. *282*, F179–F190.

Barbieri, M. A., Roberts, R. L., Gumusboga, A., Highfield, H., Alvarez-Dominguez, C., Wells, A., and Stahl, P. D. (2000). Epidermal growth factor and membrane trafficking. EGF receptor activation of endocytosis requires Rab5a. J. Cell Biol. *151*, 539–550.

Baskin, L. S., Sutherland, R. S., Thomson, A. A., Hayward, S. W., and Cunha, G. R. (1996). Growth factors and receptors in bladder development and obstruction. Lab. Investig. *75*, 157–166.

Bindels, E. M., van der Kwast, T. H., Izadifar, V., Chopin, D. K., and de Boer, W. I. (2002). Functions of epidermal growth factor-like growth factors during human urothelial reepithelialization in vitro and the role of erbB2. Urol. Res. *30*, 240–247.

Birder, L. A., Ruan, H. Z., Chopra, B., Xiang, Z., Barrick, S., Buffington, C. A., Roppolo, J. R., Ford, A. P., de Groat, W. C., and Burnstock, G. (2004). Alterations in P2X and P2Y purinergic receptor expression in urinary bladder from normal cats and cats with interstitial cystitis. Am. J. Physiol. *287*, F1084–F1091.

Chen, M. C., Solomon, T. E., Kui, R., and Soll, A. H. (2002). Apical EGF receptors regulate epithelial barrier to gastric acid: endogenous TGF-alpha is an essential facilitator. Am. J. Physiol. *283*, G1098–G1106.

Cheng, J., Huang, H., Zhang, Z. T., Shapiro, E., Pellicer, A., Sun, T. T., and Wu, X. R. (2002). Overexpression of epidermal growth factor receptor in urothelium elicits urothelial hyperplasia and promotes bladder tumor growth. Cancer Res. *62*, 4157–4163.

Chow, N. H., Liu, H. S., Yang, H. B., Chan, S. H., and Su, I. J. (1997). Expression patterns of erbB receptor family in normal urothelium and transitional cell carcinoma. An immunohistochemical study. Virchows Arch. *430*, 461–466.

Daub, H., Weiss, F. U., Wallasch, C., and Ullrich, A. (1996). Role of transactivation of the EGF receptor in signalling by G-protein-coupled receptors. Nature *379*, 557–560.

Fisher, D. A., Salido, E. C., and Barajas, L. (1989). Epidermal growth factor and the kidney. Annu. Rev. Physiol. *51*, 67–80.

Freeman, M. R., Yoo, J. J., Raab, G., Soker, S., Adam, R. M., Schneck, F. X., Renshaw, A. A., Klagsbrun, M., and Atala, A. (1997). Heparin-binding EGF-like growth factor is an autocrine growth factor for human urothelial cells and is synthesized by epithelial and smooth muscle cells in the human bladder. J. Clin. Investig. *99*, 1028–1036.

Gonnella, P. A., Siminoski, K., Murphy, R. A., and Neutra, M. R. (1987). Transepithelial transport of epidermal growth factor by absorptive cells of suckling rat ileum. J. Clin. Investig. *80*, 22–32.

Harris, R. C., Chung, E., and Coffey, R. J. (2003). EGF receptor ligands. Exp. Cell Res. *284*, 2–13.

Hecht, D., and Zick, Y. (1992). Selective inhibition of protein tyrosine phosphatase activities by H2O2 and vanadate in vitro. Biochem. Biophys. Res. Commun. *188*, 773–779.

Helin, K., Velu, T., Martin, P., Vass, W. C., Allevato, G., Lowy, D. R., and Beguinot, L. (1991). The biological activity of the human epidermal growth factor receptor is positively regulated by its C-terminal tyrosines. Oncogene *6*, 825–832.

Holbro, T., and Hynes, N. E. (2004). ErbB receptors: directing key signaling networks throughout life. Annu. Rev. Pharmacol. Toxicol. *44*, 195–217.

Huang, H., Kamm, R. D., and Lee, R. T. (2004). Cell mechanics and mechanotransduction: pathways, probes, and physiology. Am. J. Physiol. *287*, C1–C11.

Iwasaki, H., Eguchi, S., Ueno, H., Marumo, F., and Hirata, Y. (2000). Mechanical stretch stimulates growth of vascular smooth muscle cells via epidermal growth factor receptor. Am. J. Physiol. *278*, H521–H529.

Karnaky, K. J., Jr. (1998). Regulating epithelia from the apical side: new insights. Focus on "differential signaling and regulation of apical vs. basolateral EGFR in polarized epithelial cells". Am. J. Physiol. *275*, C1417–C1418.

Keay, S., Kleinberg, M., Zhang, C. O., Hise, M. K., and Warren, J. W. (2000). Bladder epithelial cells from patients with interstitial cystitis produce an inhibitor of heparin-binding epidermal growth factor-like growth factor production. J. Urol. *164*, 2112–2118.

Krepinsky, J. C., Li, Y., Chang, Y., Liu, L., Peng, F., Wu, D., Tang, D., Scholey, J., and Ingram, A. J. (2005). Akt mediates mechanical strain-induced collagen production by mesangial cells. J. Am. Soc. Nephrol. *16*, 1661–1672.

Kudoh, S., Komuro, I., Hiroi, Y., Zou, Y., Harada, K., Sugaya, T., Takekoshi, N., Murakami, K., Kadowaki, T., and Yazaki, Y. (1998). Mechanical stretch induces hypertrophic responses in cardiac myocytes of angiotensin II type 1a receptor knockout mice. J. Biol. Chem. *273*, 24037–24043.

Kuwada, S. K., Lund, K. A., Li, X. F., Cliften, P., Amsler, K., Opresko, L. K., and Wiley, H. S. (1998). Differential signaling and regulation of apical vs. basolateral EGFR in polarized epithelial cells. Am. J. Physiol. *275*, C1419–C1428.

Lax, I., Bellot, F., Howk, R., Ullrich, A., Givol, D., and Schlessinger, J. (1989). Functional analysis of the ligand binding site of EGF-receptor utilizing chimeric chicken/human receptor molecules. EMBO J. *8*, 421–427.

Lewis, S. A., and de Moura, J. L. (1982). Incorporation of cytoplasmic vesicles into apical membrane of mammalian urinary bladder epithelium. Nature *297*, 685–688.

Lewis, S. A., and de Moura, J. L. (1984). Apical membrane area of rabbit urinary bladder increases by fusion of intracellular vesicles: an electrophysiological study. J. Membr. Biol. *82*, 123–136.

Mellon, J. K., Cook, S., Chambers, P., and Neal, D. E. (1996). Transforming growth factor alpha and epidermal growth factor levels in bladder cancer and their relationship to epidermal growth factor receptor. Br. J. Cancer *73*, 654–658.

Messing, E. M. (1990). Clinical implications of the expression of epidermal growth factor receptors in human transitional cell carcinoma. Cancer Res. *50*, 2530–2537.

Milenkovic, I., Weick, M., Wiedemann, P., Reichenbach, A., and Bringmann, A. (2003). P2Y receptor-mediated stimulation of Muller glial cell DNA synthesis: dependence on EGF and PDGF receptor transactivation. Investig. Ophthalmol. Vis. Sci. *44*, 1211–1220.

Mitamura, T., Higashiyama, S., Taniguchi, N., Klagsbrun, M., and Mekada, E. (1995). Diphtheria toxin binds to the epidermal growth factor (EGF)-like domain of human heparin-binding EGF-like growth factor/diphtheria toxin receptor and inhibits specifically its mitogenic activity. J. Biol. Chem. *270*, 1015–1019.

Mount, C. D., Lukas, T. J., and Orth, D. N. (1985). Purification and characterization of epidermal growth factor (beta-urogastrone) and epidermal growth factor fragments from large volumes of human urine. Arch. Biochem. Biophys. *240*, 33–42.

Nguyen, H. T., Adam, R. M., Bride, S. H., Park, J. M., Peters, C. A., and Freeman, M. R. (2000). Cyclic stretch activates p38 SAPK2-, ErbB2-, and AT1-dependent signaling in bladder smooth muscle cells. Am. J. Physiol. *279*, C1155–C1167.

Olayioye, M. A., Neve, R. M., Lane, H. A., and Hynes, N. E. (2000). The ErbB signaling network: receptor heterodimerization in development and cancer. EMBO J. *19*, 3159–3167.

Pearson, G., Robinson, F., Beers Gibson, T., Xu, B. E., Karandikar, M., Berman, K., and Cobb, M. H. (2001). Mitogen-activated protein (MAP) kinase pathways: regulation and physiological functions. Endocr. Rev. *22*, 153–183.

Rezzonico, R. *et al.* (2003). Focal adhesion kinase pp125FAK interacts with the large conductance calcium-activated hSlo potassium channel in human osteoblasts: potential role in mechanotransduction. J. Bone Miner. Res. *18*, 1863–1871.

Rotterud, R., Nesland, J. M., Berner, A., and Fossa, S. D. (2005). Expression of the epidermal growth factor receptor family in normal and malignant urothelium. BJU Int. *95*, 1344–1350.

Sanchez-Esteban, J., Wang, Y., Gruppuso, P. A., and Rubin, L. P. (2004). Mechanical stretch induces fetal type II cell differentiation via an epidermal growth factor receptor-extracellular-regulated protein kinase signaling pathway. Am. J. Respir. Cell Mol. Biol. *30*, 76–83.

Singh, A. B., and Harris, R. C. (2005). Autocrine, paracrine and juxtacrine signaling by EGFR ligands. Cell Signal. *17*, 1183–1193.

Sun, Y., Keay, S., De Deyne, P. G., and Chai, T. C. (2001). Augmented stretch activated adenosine triphosphate release from bladder uroepithelial cells in patients with interstitial cystitis. J. Urol. *166*, 1951–1956.

Takahashi, M., Ishida, T., Traub, O., Corson, M. A., and Berk, B. C. (1997). Mechanotransduction in endothelial cells: temporal signaling events in response to shear stress. J. Vasc. Res. *34*, 212–219.

Truschel, S. T., Wang, E., Ruiz, W. G., Leung, S. M., Rojas, R., Lavelle, J., Zeidel, M., Stoffer, D., and Apodaca, G. (2002). Stretch-regulated exocytosis/endocytosis in bladder umbrella cells. Mol. Biol. Cell *13*, 830–846.

Tschumperlin, D. J. *et al.* (2004). Mechanotransduction through growth-factor shedding into the extracellular space. Nature *429*, 83–86.

Wang, E., Truschel, S., and Apodaca, G. (2003). Analysis of hydrostatic pressure-induced changes in umbrella cell surface area. Methods *30*, 207–217.

Wang, E. C., Lee, J. M., Ruiz, W. G., Balestreire, E. M., von Bodungen, M., Barrick, S., Cockayne, D. A., Birder, L. A., and Apodaca, G. (2005). ATP and purinergic receptor-dependent membrane traffic in bladder umbrella cells. J. Clin. Investig. *115*, 2412–2422.

Wiley, L. M., Wu, J. X., Harari, I., and Adamson, E. D. (1992). Epidermal growth factor receptor mRNA and protein increase after the four-cell preimplantation stage in murine development. Dev. Biol. *149*, 247–260.

Yano, S., Komine, M., Fujimoto, M., Okochi, H., and Tamaki, K. (2004). Mechanical stretching in vitro regulates signal transduction pathways and cellular proliferation in human epidermal keratinocytes. J. Investig. Dermatol. *122*, 783–790.

Yu, W., Zacharia, L. C., Jackson, E. K., and Apodaca, G. (2006). Adenosine receptor expression and function in bladder uroepithelium. Am. J. Physiol. *291*, C254–265.